JACS
JOURNAL OF THE AMERICAN CHEMICAL SOCIETY
Article
pubs.acs.org/JACS

A Mechanistic Change Results in 100 Times Faster CH Functionalization for Ethane versus Methane by a Homogeneous Pt Catalyst

Michael M. Konnick,[†] Steven M. Bischof,[†] Muhammed Yousufuddin,[‡] Brian G. Hashiguchi,*[,†] Daniel H. Ess,*[,§] and Roy A. Periana*[,†]

[†]The Scripps Energy & Materials Center, Department of Chemistry, The Scripps Research Institute, Jupiter, Florida 33458, United States

[‡]Center for Nanostructured Materials, The University of Texas at Arlington, Arlington, Texas 76019, United States

[§]Department of Chemistry and Biochemistry, Brigham Young University, Provo, Utah 84602, United States

Supporting Information

ABSTRACT: The selective, oxidative functionalization of ethane, a significant component of shale gas, to products such as ethylene or ethanol at low temperatures and pressures remains a significant challenge. Herein we report that ethane is efficiently and selectively functionalized to the ethanol ester of H_2SO_4, ethyl bisulfate ($EtOSO_3H$) as the initial product, with the Pt^{II} "Periana-Catalytica" catalyst in 98% sulfuric acid. A subsequent organic reaction selectively generates isethionic acid bisulfate ester (HO_3S-CH_2-CH_2-OSO_3H, **ITA**). In contrast to the modest 3−5 times faster rate typically observed in electrophilic CH activation of higher alkanes, ethane CH functionalization was found to be ∼100 times faster than that of methane. Experiment and quantum-mechanical calculations reveal that this unexpectedly large increase in rate is the result of a fundamentally different catalytic cycle in which ethane CH activation (and not platinum oxidation as for methane) is now turnover limiting. Facile **Pt^{II}-Et** functionalization was determined to occur via a low energy β-hydride elimination pathway (which is not available for methane) to generate ethylene and a Pt^{II}-hydride, which is then rapidly oxidized by H_2SO_4 to regenerate Pt^{II}-X_2. A rapid, non-Pt-catalyzed reaction of formed ethylene with the hot, concentrated H_2SO_4 solvent cleanly generate $EtOSO_3H$ as the initial product, which further reacts with the H_2SO_4 solvent to generate **ITA**.

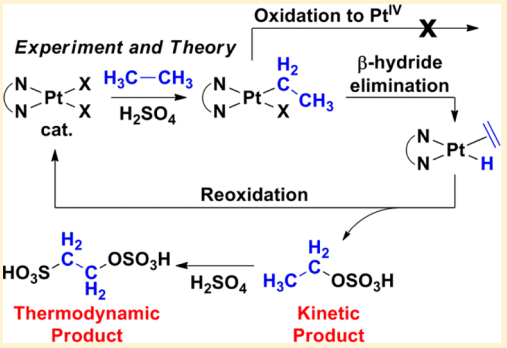

INTRODUCTION

Over the past decade there has been a significant increase in the availability of shale gas and other sources of natural gas.[1] In addition to methane, shale gas contains significant amounts of ethane.[2] Currently, the conversion of ethane to oxy-functionalized products involves multiple steps beginning with initial generation of ethylene by expensive, high-temperature (∼900 °C), capital- and energy-intensive steam cracking (Figure 1A).[3] A lower-temperature (<250 °C) selective oxidative functionalization process directly to these products could lead to substantially lower costs and reduced emissions.[4,5] One strategy that has shown promise for lower-temperature alkane conversions is based on the design of catalysts that operate via C−H bond activation[6−10] and metal−alkyl (M-R) functionalization (Figure 1B).[6,11−32]

The "Periana-Catalytica" system,[12] based on $(bpym)PtCl_2$ (bpym = 2,2′-bipyrimidine), **Pt^{II}**, which operates by CH activation in concentrated H_2SO_4 at ∼200 °C, is an efficient system for the selective catalytic conversion of CH_4 to methyl bisulfate ($MeOSO_3H$; see eq 1). Several factors led us to examine the reactions with ethane: (1) the increasing availability of ethane from shale gas; (2) the possibility that

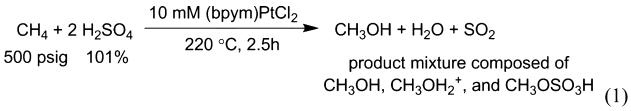

(1)

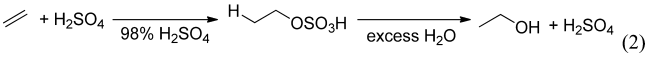

(2)

generation and separation of ethanol from ethane in sulfuric acid could be practical based upon the recognition that an early commercial process for ethanol production (albeit at lower temperatures) operated by reaction of ethylene with concentrated sulfuric acid to generate ethyl bisulfate ($EtOSO_3H$), followed by hydrolysis (eq 2);[33] (3) studies indicating that electrophilic CH activation of higher alkanes could be somewhat more reactive than that of methane (∼3−5 times),[34] which suggested that efficient ethane functionalization could be achieved at milder conditions; and (4) the presence of a β-C−H in the putative Pt-Et intermediate from C−H bond

Received: May 5, 2014

   dx.doi.org/10.1021/ja504368r | J. Am. Chem. Soc. XXXX, XXX, XXX−XXX

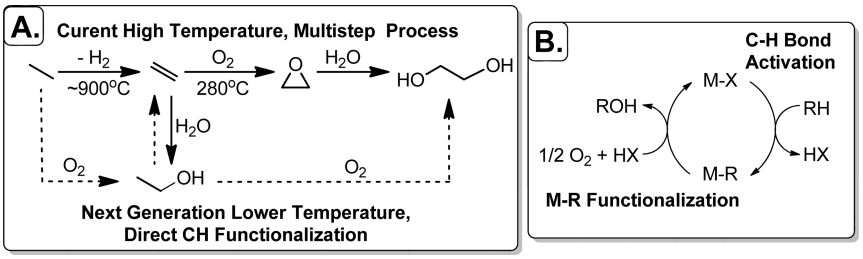

Figure 1. (A) Comparison of current multistep, high-temperature, energy- and capital-intensive processes versus a more direct approach based on lower-temperature oxidative conversion of ethane to ethylene, ethanol, and ethylene glycol. (B) Generalized catalytic cycle for hydrocarbon C−H bond functionalization.

activation, which could lead to fundamentally different chemistry for ethane relative to methane.

Herein we report that ethane undergoes selective, efficient functionalization with the Periana-Catalytica system. Functionalization proceeds by C−H bond activation to selectively generate ethyl bisulfate as the initial product with no detectable amount of C−C cleavage, over-oxidation, or decomposition (to products such as CO_2, AcOH, or intractable materials). Interestingly, rather than observing the expected further functionalization of $EtOSO_3H$ to the bis-bisulfate ester of ethylene glycol ($\mathbf{EG(OSO_3H)_2}$), the bisulfate ester of isethionic acid ($HO_3SO\text{-}CH_2CH_2\text{-}SO_3H$, referred to herein as **ITA**), which possesses a C−S and C−O bond, is cleanly generated as the final product from $EtOSO_3H$. Combined $EtOSO_3H$ and **ITA** concentrations of >1 M can be generated with >95% selectivity. Significantly, the observed 100-fold higher rate of functionalization of the CH bonds of ethane relative to methane[12] was much faster than anticipated on the basis of reported studies of electrophilic CH activation.[34] Experimental and quantum-mechanical calculations reveal that this is the result of a fundamentally different catalytic cycle as compared to that of methane functionalization. This cycle, involving ethane CH activation to generate a $\mathbf{Pt^{II}}$**-Et** intermediate, is now turnover-limiting, and $\mathbf{Pt^{II}}$**-Et** functionalization occurs by fast β-hydride elimination to generate ethylene and a $\mathbf{Pt^{II}}$**-H** intermediate, which is rapidly oxidized by hot H_2SO_4 to regenerate the active Pt catalyst. Rapid addition of H_2SO_4 to ethylene generates $EtOSO_3H$ as the initial product of the reaction, which is then converted (by a classical organic, non-Pt-mediated sulfonation reaction with the concentrated sulfuric acid solvent) into the final product, **ITA**. These results could lead to new general considerations for the design of catalysts for oxidative functionalization of higher alkanes that operate by C−H activation.

RESULTS AND DISCUSSION

Catalytic Ethane Functionalization. We began by examining ethane functionalization under conditions similar to those reported previously for methane functionalization, in 101% H_2SO_4 solvent (1 M SO_3 in 100% H_2SO_4) with 15 mM (bpym)PtX_2 (X = Cl, TFA) catalyst at 500 psig of ethane at 160 °C for 1 h in a stirred high-pressure reactor (eq 3). In

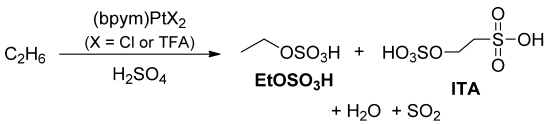

(3)

101% H_2SO_4 media, only **ITA** (and no $EtOSO_3H$) was observed. Isethionic acid ($HO\text{-}CH_2CH_2\text{-}SO_3H$, which is readily produced upon hydrolysis of **ITA**) is utilized industrially in the production of biodegradable ionic surfactants and taurine and is currently produced via (1) the reaction of aqueous $NaHSO_3$ with ethylene oxide or (2) the sulfonation and subsequent hydrolysis of ethylene.[35,36] To avoid complications from possible formation of chlorination products, subsequent studies were carried out with (bpym)$Pt(TFA)_2$, **1**. Significantly, carrying out the reaction with **1** in 98% H_2SO_4 under otherwise identical conditions showed formation of both $EtOSO_3H$ and **ITA** (in a 1:1.7 ratio, respectively) as the only products. This suggested that $EtOSO_3H$ could be the initial product, which is then subsequently converted into **ITA**. However, given the long-known rapid conversion of ethylene to $EtOSO_3H$ in concentrated H_2SO_4 solvent,[33] it is also possible that the initial product of the reaction is ethylene, which would not be observed. This result is significant, as if the system could be modified to selectively generate $EtOSO_3H$ as the major product, it could be possible to isolate EtOH by the procedures developed in the early commercial synthesis of EtOH based on reaction of ethylene with 98% H_2SO_4.[33]

Catalysis with **1** was efficient and highly selective; in 101% H_2SO_4 with 15 mM **1** at 160 °C for 2.5 h, **ITA** concentrations of >1 M were observed. After the reactions were completed, the solution phase remained homogeneous. No other C_2 products (such as CH_3CO_2H, CH_3CHO, or $CH_3CH_2\text{-}SO_3H$), were observed. Consistent with catalysis by a (bpym)Pt complex, control experiments show that **1** was required for reaction, and no reaction was observed with bpym ligand, trifluoroacetate anions, Pt black, insoluble $PtCl_2$, or soluble K_2PtCl_4 under otherwise identical conditions. Importantly, no C_1 side-products (such as CH_3OSO_3H, CH_3SO_3H, CH_3OH, CH_3TFA, or HCO_2H), were observed. To more rigorously examine reaction selectivity, the reaction was carried out with 100% $^{13}C_2H_6$ in 98% H_2SO_4 solvent. Analysis of the liquid phase by ^1H and ^{13}C NMR spectroscopy, and the gas phase by GC-MS, showed only $^{13}CH_3{}^{13}CH_2\text{-}OSO_3H$ (^{13}C-$EtOSO_3H$) and $HO_3SO\text{-}^{13}CH_2{}^{13}CH_2\text{-}SO_3H$ (^{13}C-**ITA**) as the products. Alternative potential products, such as $^{13}C_2H_4$, $^{13}CH_3{}^{13}CH_2SO_3H$, $^{13}CH_3{}^{13}CO_2H$, or $^{13}CO_2$, were not observed. Additionally, control studies show that added **ITA** is essentially inert to over-oxidation to generate CO_2 or other products under catalytic conditions (see Supporting Information (SI), Table S1). Consistent with the reaction products shown above (eq 3), gas-phase analysis (via quantitative analytical titration, see Experimental Section below) indicated that a substantial amount of SO_2 is generated during the reaction.

dx.doi.org/10.1021/ja504368r | J. Am. Chem. Soc. XXXX, XXX, XXX−XXX

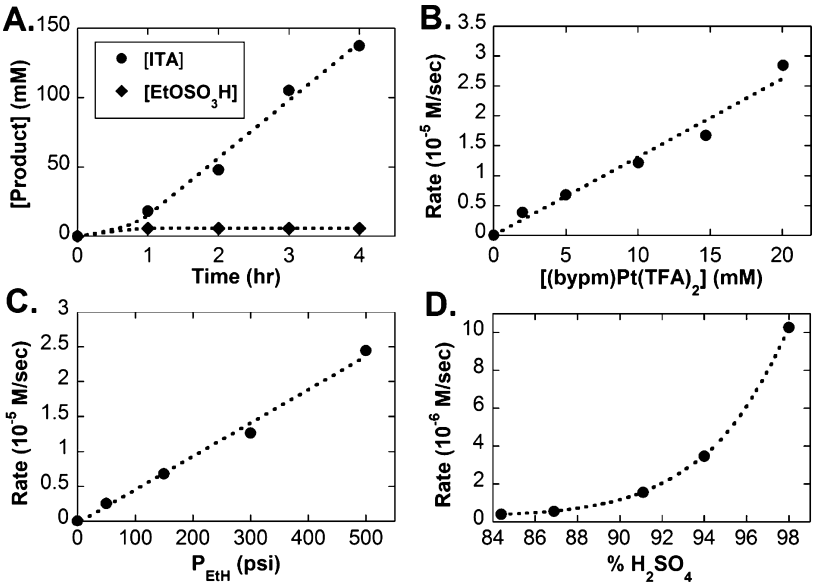

Figure 2. Reaction time course (A), initial rate [Pt^{II}] dependence (B), EtH pressure dependence (C), and % H_2SO_4 dependence (D) for the oxidation of EtH catalyzed by **1**. Reaction conditions: (A) 5 mM **1**, 150 psi EtH, 3 mL of 98% H_2SO_4, 1−4 h, 160 °C; (B) 2−20 mM **1**, 150 psi EtH, 3 mL of 98% H_2SO_4, 1 h, 160 °C; (C) 5 mM **1**, 50−500 psi EtH, 3 mL of 98% H_2SO_4, 1 h, 160 °C; (D) 5 mM **1**, 150 psi EtH, 3 mL of 84−98% H_2SO_4, 3 h, 160 °C.

The observed functionalization of ethane is significant for several reasons. First, the reaction with ethane is highly selective in generating $EtOSO_3H$ and **ITA** as the *only* observed products. Second, in contrast to MeH (where no C−S products, such as CH_3SO_3H, were observed), the EtH functionalization product **ITA** contains both C-SO_3H and C-OH functional groups. Third, ethane functionalization is substantially more facile than methane functionalization, as comparable conversions were observed at much lower temperatures than previously reported for methane (160 vs 220 °C, respectively). These observations suggested the possibility for a reaction mechanism different than that previously determined for methane and prompted our more detailed analysis, presented below.

Reaction Pathway for ITA Production. To more rigorously examine the mechanism of ethane oxidation catalyzed by **1**, we studied the reaction kinetics under milder conditions using 98% H_2SO_4 solvent at 160 °C. As can be seen in Figure 2A (see SI for data), a reaction time course indicated an unchanging, steady-state [$EtOSO_3H$] throughout the reaction with a linear growth of [**ITA**]. This data is consistent with the generation of $EtOSO_3H$ (or ethylene, *vide supra*) as the initial observed product, which is converted to **ITA** as the final, stable product. All reactions were shown to be highly reproducible, and initial rates studies indicate a first-order dependence on both the concentration of **1** and ethane pressure (Figure 2B, 2C). Similar to our previous studies on the system with methane, the reaction rate is highly dependent upon the concentration of H_2SO_4 and asymptotically decreases at lower concentrations of H_2SO_4 (Figure 2D). Interestingly, while lower ethane conversions are observed, the product ratios *increasingly favor* $EtOSO_3H$ over **ITA** as the concentration of H_2SO_4 is decreased (see SI, Figure S4). This would suggest that the rate of conversion of $EtOSO_3H$ into **ITA** increases with increasing concentration of H_2SO_4.

Both $EtOSO_3H$ and ethylene were shown in very early as well as later studies by others to readily react by a classical organic reaction in concentrated H_2SO_4 or oleum to cleanly generate **ITA**.[37−44] The reaction mechanism for the conversion of $EtOSO_3H$ to **ITA** has been proposed to involve reversible formation of ethylene (by elimination of H_2SO_4 from $EtOSO_3H$) followed by addition of the S−O bond of disulfuric acid (e.g., $H_2S_2O_7$, which is known to be present in concentrated H_2SO_4 solutions)[45−47] across ethylene, resulting in both C−S and C−O bond formation to generate **ITA** (Scheme 1).[38−43] To examine the possibility of $EtOSO_3H$ as a precursor to **ITA** under catalytic conditions, the reactions of $EtOSO_3H$ with concentrated sulfuric acid were examined in the presence and absence of **1**. Consistent with a prior report,[37,38,44] in both 101% and 98% H_2SO_4 media at 160 °C, $EtOSO_3H$ was converted into **ITA** as the sole product (see SI, Table S1). Significantly, identical results were obtained in the presence or absence of **1**, indicating that catalysis by Pt is not necessary for $EtOSO_3H$-to-**ITA** transformation. The reaction is faster in 101% H_2SO_4, but **ITA** is the final product in both cases with >90% mass balance.

Scheme 1. Proposed Pathways and Relative Rates for the Conversion of Ethane to $EtOSO_3H$ and ITA

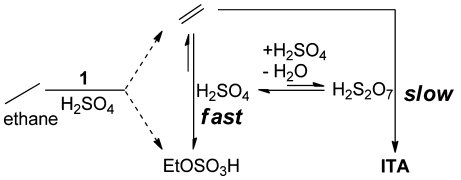

Consistent with earlier reports,[37,38,44] replacing $EtOSO_3H$ with ethylene showed identical results and conversion into primarily **ITA** with some $EtOSO_3H$ in <1 h at 160 °C in the presence or absence of Pt (Figure 3A). Lowering the temperature slightly (ca. 140 °C, Figure 3B) allowed us to observe a mixture of both **ITA** and $EtOSO_3H$. Consistent with the very early literature,[32,33] and the possibility of reversible generation of ethylene from $EtOSO_3H$, we confirmed that ethylene is quantitatively converted solely into $EtOSO_3H$ in 1 h at 50 °C (Figure 3C). These results, as well as the kinetic

dx.doi.org/10.1021/ja504368r | J. Am. Chem. Soc. XXXX, XXX, XXX−XXX

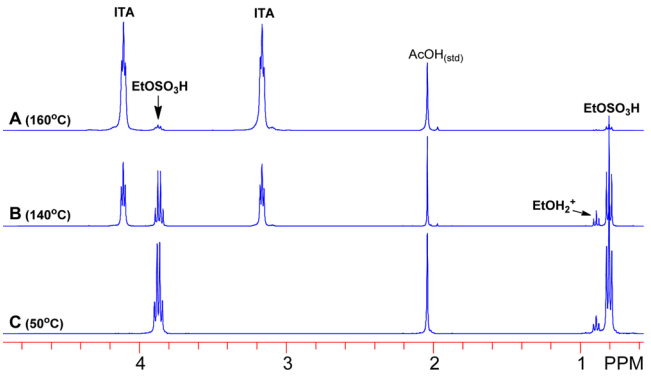

Figure 3. ^{1}H NMR of 98% H_2SO_4 after exposure to C_2H_4 for 1 h at (A) 160, (B) 140, and (C) 50 °C.

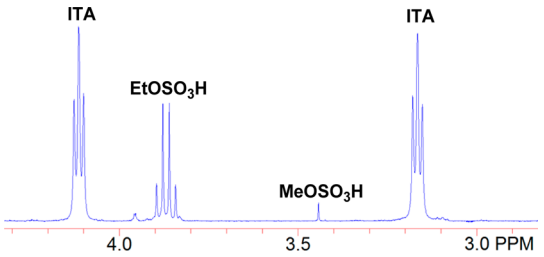

Figure 4. ^{1}H NMR of the post-reaction mixture with a 1:1 mixture of methane to ethane. Reaction conditions: 15 mM **1**, 250 psi MeH/250 psi EtH (500 psi total pressure), 3 mL of 98% H_2SO_4, 1 h, 160 °C.

profiles shown above (Figure 2), are consistent with the reactions of ethane catalyzed by **1**, generating either ethylene or $EtOSO_3H$ as the initial product, followed by conversion to **ITA** (Scheme 1).

Mechanism of Ethane Functionalization. Given the expected similarities of methane and ethane,[32,34] we anticipated that functionalization of ethane catalyzed by **1** produces $EtOSO_3H$ and **ITA** via a C−H activation mechanism. However, it is also possible that free radical reactions are involved. Sen and co-workers had previously reported that the non-transition metal-mediated oxidation of ethane in either 98% H_2SO_4 or oleum with radical initiators ($Ce(SO_4)_2$ or $K_2S_2O_8$) generated **ITA** at ∼5% selectivity with predominantly C_1 products (via C−C bond cleavage) and over-oxidation products such as CH_3CO_2H.[26,44,48] The poor selectivity for **ITA**, generation of C−C bond cleavage products, and over-oxidized products led Sen and co-workers to propose a mechanism involving free-radical chain reactions initiated by $K_2S_2O_8$. Since C_1 and over-oxidized products are not observed in our work on the selective functionalization of ethane described above, we considered a radical chain mechanism unlikely. Additionally, the well-defined and reproducible kinetic data, along with no induction period and lack of side products, strongly support our proposal for a nonradical mechanism based on ethane CH activation.

To further examine the similarities between the reactions of methane and ethane with **1**, we examined the relative rates of functionalization through competition reactions. Competition studies were carried out in 98% H_2SO_4 solvent containing **1** at identical pressures of methane and ethane, under conditions where the reactions were not mass transfer limited and at <10% conversion of both alkanes to ensure pseudo-first-order conditions. Unexpectedly, the amount of the C_2 products ($EtOSO_3H$ + **ITA**) produced from ethane functionalization *was found to be ∼144 times higher* (suggesting a ∼100-fold higher rate when correcting for the number of CH bonds) than the amound of $MeOSO_3H$ from methane functionalization (Figure 4). This was much higher than anticipated on the basis of reported rates of electrophilic CH activation of various hydrocarbons.[34]

We recently showed that one of two plausible pathways for methane functionalization in the Periana-Catalytica system (Scheme 2, red cycle, R = Me) involves fast C−H activation to reversibly generate a (bpym)Pt^{II}-Me intermediate (k_1), followed by reaction with of non-methylated Pt^{IV} that is generated by the turnover-limiting step, oxidation of non-methylated Pt^{II} to Pt^{IV} (k_4) *that does not involve methane*.[32] Thus, if ethane reacted by this mechanistic pathway (Scheme 2, red cycle, R = Et), comparable rates of reaction of ethane and methane could be anticipated. The ∼100-fold difference in reaction rates observed between these alkanes suggested that ethane functionalization may occur by a fundamentally different mechanism. One plausible mechanism for the functionalization of ethane is shown below (Scheme 2, blue cycle, R = Et). Analogous to the methane functionalization cycle, the ethane cycle begins with the C−H activation step of ethane by $\mathbf{Pt^{II}}$ to generate a $\mathbf{Pt^{II}}$**-Et** intermediate, k_2. At this point the ethane and methane mechanisms diverge. Unlike the analogous $\mathbf{Pt^{II}}$**-Me** intermediate, the $\mathbf{Pt^{II}}$**-Et** intermediate could be expected to undergo facile β-hydride elimination to give a $\mathbf{Pt^{II}(H)(C_2H_4)}$ intermediate (k_5). Subsequent loss of ethylene (k_6) and known reversible addition of H_2SO_4 or irreversible addition of $H_2S_2O_7$ to ethylene give $EtOSO_3H$ or **ITA**, respectively.[37,38,44] It is also possible that these functionalization reactions could occur on the ethylene coordinated to Pt (see SI, Figure S8). However, since control reactions show that **1** is not required for the conversion of ethylene to $EtOSO_3H$ and **ITA**, *vide supra*, catalysis by **1** for ethylene conversion is not required to explain the observed results. The $\mathbf{Pt^{II}}$**-H** is then oxidized by H_2SO_4 to generate SO_2 and regenerate the $\mathbf{Pt^{II}}$ catalyst (k_7). Although β-hydride elimination is widely known to occur in M-R complexes,[49,50] in catalytic systems for alkane functionalization it has been utilized almost exclusively for generating alkenes as the final products.[51] If this proposed mechanism is correct (Scheme 2, blue cycle), it would describe a high-yielding catalytic system for alkane oxy-functionalization involving a β-hydride elimination step which leads to products with C−O bonds. In order to examine this mechanistic possibility, further studies were undertaken as described below.

C−H Activation Step. Catalytic H/D exchange with alkane substrates in D-acids is commonly utilized to provide evidence for C−H activation by reversible generation of a M-R intermediate. To examine this, we carried out the catalytic reaction of ethane with **1** in 98% D_2SO_4 160 °C. Consistent with a C−H activation mechanism involving generation of **Pt-Et**, deuterated ethane (D-ethane) was generated along with partially deuterated $EtOSO_3H$ and **ITA**. While highly accurate quantitative analysis of the products when utilizing 98% D_2SO_4 was complicated by the formation of several ethane isotopologs ($C_2H_nD_{6-n}$) and D-incorporation into the oxidized products ($EtOSO_3H$ and **ITA**), we found approximately a 1:1 molar ratio of $C_2H_nD_{6-n}$ to oxidized products. On the basis of our proposed mechanism above (Scheme 2, blue cycle), this ratio would result from the branching rates from reaction of $\mathbf{Pt^{II}}$**-Et** with D_2SO_4 to generate D-ethane versus the functionalization reaction of $\mathbf{Pt^{II}}$**-Et** to generate $EtOSO_3H$ and **ITA** (k_{-1}/k_6, R = Et, see SI). Importantly, the 1:1 ratio of D-ethane to $EtOSO_3H$/**ITA** for ethane starkly contrasts with the reported

dx.doi.org/10.1021/ja504368r | J. Am. Chem. Soc. XXXX, XXX, XXX−XXX

Scheme 2. Proposed Catalytic Cycles for the Functionalization of Methane (Red) and Ethane (Blue) by (bpym)Pt(TFA)$_2$, 1, in H_2SO_4

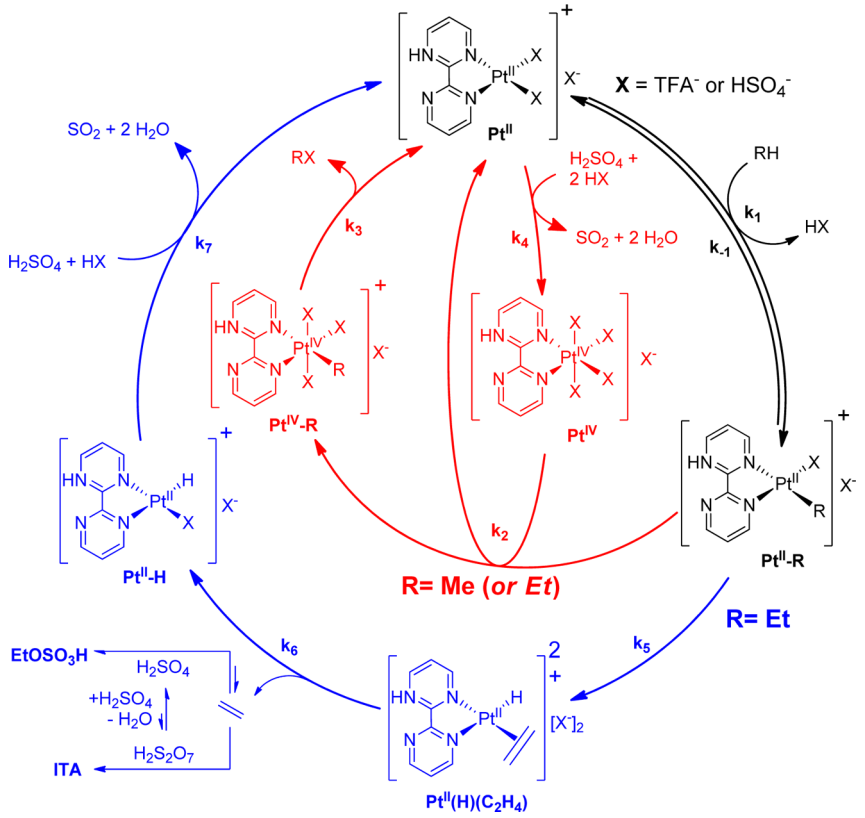

~20:1 ratio of D-methane to functionalized product from reactions of methane catalyzed by **Pt^{II}** (k_{-1}/k_2, R = Me).[32] This substantial difference in the ratio of products from catalysis with **1** in D_2SO_4 provides further evidence that, while methane and ethane substrates could both undergo C−H activation with **Pt^{II}**, the functionalization steps for the **Pt^{II}-R** intermediates (R = Me and Et) are different.[52]

Pt-Ethyl Functionalization. To examine the **Pt^{II}-Et** functionalization step (k_5) in more detail, the complex (bpym)Pt^{II}(Et)(TFA), **2**, was synthesized and fully characterized (Figure 5, see SI) and examined as a model for the **Pt^{II}-Et** intermediate. Based on the reaction mechanism shown above (Scheme 2), kinetic analysis, and the ~1:1 ratio of D-ethane to $EtOSO_3H$ and **ITA** from the catalytic reaction of ethane with **1** in D_2SO_4 solvent at 160 °C, a branching ratio of ~1:1 for ethane to functionalized product was expected from the stoichiometric reaction of **2** with D_2SO_4 solvent at the same temperature. The stoichiometric reactivity of **2** was examined under the catalytic conditions (but in the absence of ethane) by adding 100 μL of a 1 M solution of **2** in DMSO all at once to 5.0 mL of a stirred solution of 98% H_2SO_4 at 160 °C in a sealed glass vial under Ar (Scheme 3). The vial was removed and allowed to cool to room temperature immediately after addition of **2**. The gas phase and liquid phase after reaction were analyzed by GC-MS and NMR, respectively (see SI for specific details and controls for this procedure). This reaction showed the formation of $EtOSO_3H$ and ethane in 65% and 35% yields, respectively, based on added **2** (Table 1, entry 1).

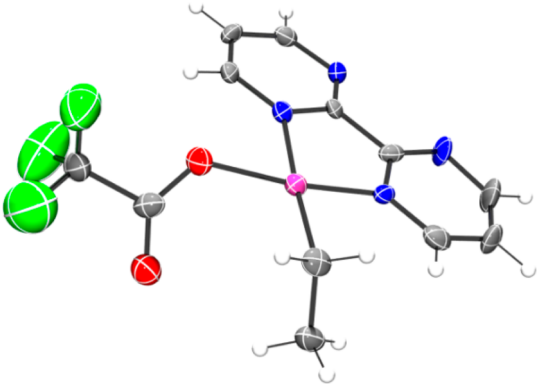

Figure 5. ORTEP structure of (bpym)Pt(Et)(TFA), **2**, with 30% probability ellipsoids.

Scheme 3. Functionalization and Protonolysis of (bpym)Pt^{II}(Et)(TFA), 2, upon Addition to 98% H_2SO_4 at 160 °C

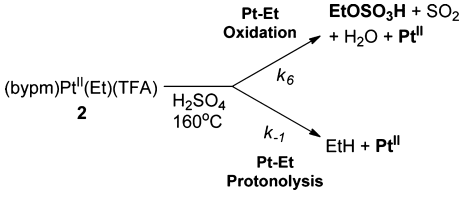

Significantly, consistent with the proposed oxidation of a putative **Pt^{II}-H** intermediate, k_7, functionalization is accompanied by oxidation with H_2SO_4, as 1 equiv of SO_2 relative to $EtOSO_3H$ was also generated (see Experimental Section for details). Consistent with the high selectivity of the reaction and

dx.doi.org/10.1021/ja504368r | J. Am. Chem. Soc. XXXX, XXX, XXX−XXX

Table 1. Reaction of (bpym)Pt^{II}(R)(TFA), 2 and 3, in HX at 160 °C[a]

entry	Pt(bpym)(TFA)-R	acid	RX (%)	RH (%)
1	R = Et (**2**)	H_2SO_4	65	35
2	R = Me (**3**)	H_2SO_4	5	95
3	R = Et (**2**)	HOTf	15	80
4	R = Me (**3**)	HOTf	0	100

[a]Reactions were carried out at 160 °C in 98% H_2SO_4 or neat HOTf with 10 mM **2** or **3**.

the absence of any stable intermediates or side products, mass balance of >90% based on **2** was observed. Importantly, no **ITA** was observed at this short reaction time, and $EtOSO_3H$ was observed as the sole product. This is consistent with studies, *vide supra*, that show that while $EtOSO_3H$ is converted to **ITA** under the reaction conditions, conversion is not instantaneous. Within the experimental error, this molar ratio of ethane to $EtOSO_3H$ is comparable to the ∼1:1 molar ratio of D-ethane (in D_2SO_4) to the total number of moles of $EtOSO_3H$ and **ITA** (in H_2SO_4) obtained from the functionalization of ethane by H_2SO_4 catalyzed by **1**. Consistent with a different mechanism for reactions with methane, previous studies showed that the stoichiometric reaction of (bpym)Pt^{II}(Me)(TFA), **3** (a model of **Pt^{II}-Me**), in H_2SO_4 showed primarily CH_4 generated by protonolysis and almost no $MeOSO_3H$ formation that would be anticipated for functionalization of **Pt^{II}-Me** with H_2SO_4 (Table 1, Entry 2).[32] These observations provide further evidence for the alternate mechanism shown above (Scheme 2, blue cycle, R = Et) involving reversible C−H bond activation of ethane to generate **Pt^{II}-Et**, followed by functionalization. Significantly, these results would suggest that, unlike the methane system where oxidation of Pt^{II} to Pt^{IV} is the slow step, the turnover-limiting step in the case of ethane is CH activation, k_1, R = Et.

In addition to the β-hydride elimination step (Scheme 2, k_6), **Pt^{II}-Et** functionalization requires two additional steps: (i) functionalization of ethylene to give $EtOSO_3H$ and **ITA**, which can occur by ethylene dissociation (Scheme 2, k_6), followed by non-Pt-catalyzed, classical reversible addition of H_2SO_4 and sulfonation with $H_2S_2O_7$, and (ii) **Pt^{II}-H** oxidation to generate SO_2 (Scheme 2, k_7). To account for the ∼1:1 ratio of branching rates for protonolysis and functionalization from **Pt^{II}-Et**, the rate of step k_5 must be comparable to k_{-1}, and step k_6 must be comparable to or faster than re-formation of **Pt^{II}-Et** by olefin insertion on **$Pt^{II}(H)(C_2H_4)$**, k_{-6} (not shown). Additionally, to account for the formation of 1 equiv of SO_2 in the stoichiometric reaction of **2** with D_2SO_4, step k_7 step must also be comparable to or faster than k_5.

However, the above result does not rule out the possibility that β-hydride elimination and oxidation by H_2SO_4 to generate SO_2 occur in a single step with no discrete **Pt^{II}-H** intermediate and that is competitive with k_{-1}. Another alternative, though we consider this unlikely based on reactions of the **Pt^{II}-Me** model complex (*vide infra*), is the direct oxidation and functionalization of **Pt^{II}-Et** by H_2SO_4 to generate $EtOSO_3H$ without the involvement of a β-hydride elimination step (k_2, Scheme 2, red cycle, R = Et). Since these alternative mechanisms both require oxidation by H_2SO_4 to generate $EtOSO_3H$ from **Pt^{II}-Et**, we examined the reaction of **2** in neat CF_3SO_3H, a non-oxidizing acid, under conditions similar to those of the reaction with H_2SO_4. Significantly, both the ethyl ester, CF_3SO_3Et, and ethane were formed in this reaction in ∼15% and ∼80% yields, respectively, based on added **2** (Table 1, entry 3). Importantly, no Pt-black (Pt^0) or SO_2 was observed. While the molar ratio of these products (∼1.5:8) is different from that found in H_2SO_4 (∼2:1), CF_3SO_3H is a stronger acid than H_2SO_4, and more protonolysis of **2** to generate ethane is expected. These observations show that oxidation of **Pt^{II}-Et** by H_2SO_4 to give SO_2 is not required for **Pt^{II}-Et** functionalization to generate $EtOSO_3H$, *in stark contrast to* ***Pt^{II}-Me*** *functionalization.*

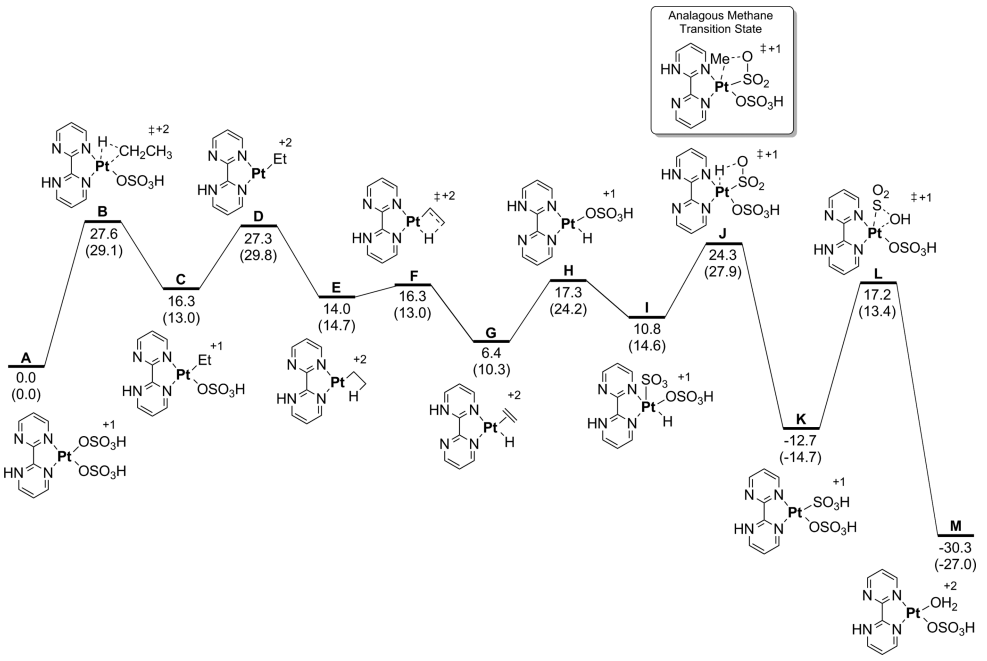

Figure 6. B3LYP free energy surface for ethane C−H activation, β-hydride elimination, and Pt-hydride oxidation. M06 free energies are given in parentheses. Energies are reported in kcal/mol.

dx.doi.org/10.1021/ja504368r | J. Am. Chem. Soc. XXXX, XXX, XXX−XXX

Consistent with this difference between methane and ethane, the reaction of the **Pt^{II}-Me** model, **3**, in non-oxidizing CF_3SO_3H (Table 1, entry 4) generated only methane; no MeOTf was observed within the limits of detection. Analysis of the mixture after reaction of **Pt^{II}-Et** in CF_3SO_3H showed no detectable **Pt^{II}-H** intermediate. However, this does not rule out the possibility of **Pt^{II}-H** intermediacy, since previous studies of **Pt^{II}-Me** species in H_2SO_4 solvent showed that rapid proton exchange with the ligands and anions of the Pt complex led to ill-defined and very broad resonances. It is also possible that protonolysis of **Pt^{II}-H** generates H_2 that we could not identify. Attempts at synthesizing and characterizing $[Pt^{II}(H)(C_2H_4)]^+[TFA]^-$ as a model of **$Pt^{II}(H)(C_2H_4)$** were unsuccessful, likely due to the instability of the complex. These results provide strong support for our proposed mechanism involving β-hydride elimination, loss of ethylene (that reacts with CF_3SO_3H to generate CF_3SO_3Et), and generation of a **Pt^{II}-H** intermediate.

Computational Analysis. We have also performed density functional theory (DFT) calculations to examine the proposed catalytic mechanism (Figure 6). These calculations are also consistent with CH activation as the turnover-limiting step in the functionalization of ethane catalyzed by **1**. Similar to the computed methane functionalization mechanism,[53−56] we identified a pathway involving ethane coordination and C−H bond cleavage by $[(H\text{-bpym})Pt^{II}(OSO_3H)_2]^+$, **A** (**$Pt^{II}$**), the presumed active catalyst in H_2SO_4. The B3LYP $\Delta G^{\ddagger}$ for C−H activation via transition state **B** is 27.6 kcal/mol, leading to the generation of the Pt-ethyl intermediate, **C** (**Pt^{II}-Et**). This endergonic intermediate (ΔG = 16.3 kcal/mol) is consistent with the observed H/D exchange with ethane and D_2SO_4 that would be expected from reversible formation of **C**. From **C**, loss of a bisulfate ligand to give the tri-coordinate species **D** thermodynamically requires ΔG = 27.3 kcal/mol. An intramolecular agostic interaction between the ethyl group and the Pt metal center (structure **E**) occurs prior to facile β-hydride elimination via transition state **F** with $\Delta G^{\ddagger}$ = 16.3 kcal/mol to give the Pt-hydride ethylene complex **G** (**$Pt^{II}(H)(C_2H_4)$**) with ΔG = 6.4 kcal/mol. From complex **G**, dissociation of ethylene followed by bisulfate coordination gives complex **H** (**Pt^{II}-H**), which thermodynamically requires ΔG = 17.3 kcal/mol. As shown experimentally above (Figure 3), ethylene would then be rapidly converted into $EtOSO_3H$ (and subsequently **ITA**) by the hot H_2SO_4 solvent. Additionally, calculations also suggest that at Pt meditated pathway is also energetically viable, via direct functionalization of the Pt-bound ethylene species **G** (see SI for details).

Importantly, transition state **B** and intermediate **D** are close in relative free energies, which is in accord with experiments showing competitive protonolysis versus Pt-ethyl group functionalization when the model of **Pt^{II}-Et**, complex **2**, was treated with H_2SO_4. Another key feature of our proposed catalytic cycle is the fast regeneration of **Pt^{II}**, $(bpym)Pt^{II}(OSO_3H)_2$, from the Pt-hydride intermediate, **H**. Indeed, our calculations have identified several low-energy Pt-hydride oxidation mechanisms. One pathway involves SO_3 coordination to intermediate **H** to give intermediate **I** with ΔG = 10.8 kcal/mol (generation of SO_3 from concentrated H_2SO_4 is calculated to be endergonic by ∼10 kcal/mol). From **I** there is a low-energy pathway that first involves turnstile ligand rearrangement followed by transition state **J** with $\Delta G^{\ddagger}$ = 24.3 kcal/mol for proton transfer to an oxygen atom of the SO_3 group. Transition state **J** leads to the exergonic intermediate **K** (ΔG = −12.7 kcal/mol). Subsequent SO_2 extrusion via transition state **L** ($\Delta G^{\ddagger}$ = 17.2 kcal/mol) and Pt−OH protonation gives the aqua complex **M** prior to regenerating $(bpym)Pt^{II}(OSO_3H)_2$, **A** (**Pt^{II}**).

A critical feature of the energy landscape shown is that the $\Delta G^{\ddagger}$ for Pt-hydride oxidation (**G** → **K**) is lower than that computed for the C−H activation step (**A** → **C**). As noted previously, stoichiometric reaction of **2** with H_2SO_4 gave a mixture of ethane and $EtOSO_3H$. In contrast, stoichiometric reaction of **TFA-Pt^{II}-Me** showed predominantly CH_4 and almost no $MeOSO_3H$. Consistent with these experiments, the computed transition state for the oxidation of Pt^{II}-methyl by SO_3 (Figure 6, inset), analogous to that for the oxidation of the Pt^{II}-hydride species **H**, was found to be ∼6 kcal/mol higher ($\Delta G^{\ddagger}$ = 30.1 kcal/mol), since proton transfer is more facile than methyl group transfer.

CONCLUSION

In summary, we have shown that ethane is functionalized rapidly and selectively to $EtOSO_3H$ as the initial product at rates that are ∼144 times higher (∼100 per CH bond) than for methane with the Periana-Catalytica system. $EtOSO_3H$ is converted to **ITA**, the final product, by a well-established, non-metal-mediated electrophilic sulfonation of ethylene (reversibly generated from $EtOSO_3H$) in concentrated sulfuric acid media. Our studies show that the faster rate of ethane functionalization to $EtOSO_3H$ (compared to methane to $MeOSO_3H$) is the result of a fundamentally different mechanism that results in much faster functionalization of **Pt^{II}-Et** compared to **Pt^{II}-Me**. Experiments and calculations have provided evidence that ethane functionalization involves turnover-limiting C−H bond activation (albeit the activation barrier is only slightly lower), followed by fast β-hydride elimination, ethylene functionalization, and Pt-hydride oxidation. This fundamentally different mechanistic pathway could help to guide new catalyst designs for the functionalization of higher-order alkanes which operate by C−H bond activation, as (1) it could be possible to generate ethanol from reactions of ethane with H_2SO_4 as the oxidizing agent if the reaction could be optimized for the formation of $EtOSO_3H$ (by designing catalysts that can operate at lower temperatures in concentrated H_2SO_4); (2) it may be possible to trap and functionalize alkene intermediates to a wide range of products; and (3) oxidation of the M-H complex should occur more readily than that of a corresponding M-R complex, potentially with a wider scope of oxidants.

EXPERIMENTAL SECTION

General Procedures. All manipulations were carried out using an argon-filled MBraun glovebox and standard Schlenk techniques using over-dried glassware (>1 h at 110 °C under vacuum, −30 mmHg) unless otherwise stated. H_2O was degassed and stored under argon before use. Reagent-grade chemicals and solvents were purchased from Sigma-Aldrich, Alfa Aesar, or EMD and used as received unless otherwise specified. 2,2′-Bipyrimidine (bpym) was purchased from Sigma-Aldrich. Deuterated solvents were purchased from Cambridge Isotope Inc. and degassed and stored under argon before use unless otherwise noted. Electrospray ionization (ESI) mass spectroscopy was performed at the University of Illinois at Urbana−Champaign Mass Spec Facility (Urbana, IL) on a Q-Tof Ultima mass spectrometer. Liquid-phase organic products were analyzed with a Shimadzu QP2010S gas chromatograph−mass spectrometer equipped with a cross-linked RTX-5 methyl silicone gum capillary column. Gas measurements were performed using an Agilent GasPro or HP Q-plot column. The retention times of the products were confirmed by

dx.doi.org/10.1021/ja504368r | J. Am. Chem. Soc. XXXX, XXX, XXX−XXX

comparison with known standards. NMR spectra were obtained on a Bruker Digital Avance III 400 spectrometer (400.132 MHz for ^{1}H, 100.623 MHz for ^{13}C, and 376.461 MHz for ^{19}F). Chemical shifts are given in ppm relative to residual solvent resonances (^{1}H and ^{13}C) or to an external capillary containing neat HTFA (δ = −76.55, ^{19}F). Pt(bpym)Cl_2[32,57−59] and diethyl(1,5-cyclooctadiene)platinum(II) (Pt-(cod)Et_2)[60] were synthesized via previously reported procedures.

Preparation of (bpym)Pt(TFA)$_2$, 1. The complex (bpym)$PtCl_2$ (468.0 mg, 1.103 mmol) was charged to a 30 mL reaction vial with 5 mL of HTFA and a magnetic stir bar. AgTFA (487.5 mg, 2.207 mmol, 2.00 equiv) was dissolved into 20 mL of HTFA, and this solution was added all at once to the HTFA suspension of (bpym)$PtCl_2$. Almost immediately a color change of the reaction mixture from burnt orange to yellow occurred, with dissolution of (bpym)$PtCl_2$ and the formation of a fine white precipitate. The reaction mixture was sonicated periodically for the next hour and then allowed to stir in the dark overnight at room temperature. The reaction mixture was filtered through a Celite plug to remove the formed AgCl, and the solid was washed three times with HTFA (5 mL). The combined HTFA filtrates were poured into 250 mL of diethyl ether, inducing the formation of a yellow precipitate. The solution was allowed to stand for 30 min to complete precipitation, and then the solid was collected via filtration, washed with excess Et_2O, and dried under vacuum overnight to yield **1** as a fine, bright yellow powder: 571 mg (89%). ^{1}H NMR spectroscopic analysis of **1** indicated that the TFA groups remained bound when examined in d_6-acetone solution; however, in CD_3CN, moderate dissociation of TFA to generate (presumably) [(bpym)Pt(TFA)-(CD_3CN)][TFA] was observed (∼20%). ^{1}H NMR (d_6-acetone, 400 MHz): δ 9.49 (dd, J = 4.8 Hz, J = 2.0 Hz, 2H), 8.95 (dd, J = 5.6 Hz, J = 2.0 Hz, 2H), 8.12 (dd, J = 5.6 Hz, J = 4.8 Hz, 2H). ^{1}H NMR (CD_3CN, 400 MHz): for **1**, δ 9.28 (dd, 2H), 8.79 (dd, 2H), 7.83 (2H); for [(bpym)Pt(TFA)(CD3CN)][TFA], δ 9.36 (dd, 1H), 9.34 (dd, 1H), 9.07 (1H), δ 8.75 (dd, 1H), 7.95 (dd, 1H), 7.88 (dd, 1H). ^{13}C{^{1}H} NMR (d_6-acetone, 100 MHz): δ 163.27 (C_{bpyz}), 162.35 (q, TFA, $^{2}J_{CF}$ = 37 Hz), 161.54 (C_{bpyz}), 157.12 (C_{bpyz}), 125.65 (C_{bpyz}), 115.77 (q, TFA, $^{1}J_{CF}$ = 289 Hz). ^{19}F NMR (d_6-acetone, 376.5 MHz): δ −72.79 (s). HRMS(ES): calcd for [M−TFA]$^+$ 466.0091, found 466.0107. Anal. Calcd for $C_{12}H_6F_6N_4O_4Pt$: C, 24.88; H, 1.04; N, 9.67. Found: C, 24.96; H, 1.10; N, 9.77.

Preparation of (bpym)PtEt_2. We followed a previously published procedure[61] with minor modifications, as our complex was not stable when subjected to the published purification procedure. A solution of 2,2′-bipyrimidine (0.44 g, 2.8 mmol) in acetonitrile (50 mL) was added to a solution of (cod)$PtEt_2$ (1.0 g, 2.8 mmol) in acetonitrile (10 mL) at room temperature. The solution began to turn red immediately and was stirred at 55 °C for 16 h. After cooling, all solvents were removed on a rotary evaporator, leaving a dark red solid. The residue was dissolved in 8 mL of CH_2Cl_2 and added to 30 mL of pentane. A dark red solid precipitated from solution, the slurry was centrifuged, and the supernatant was removed. The recrystallization procedure was repeated once more, followed by washing with pentane (3 × 30 mL). Drying under high vacuum gave 870 mg (76% yield) as a dark red powder. Attempts to obtain elemental analysis were unsuccessful, as residual bpym ligand (∼5 mol %) remained in the ^{1}H NMR. This compound was taken on to the next step without further purification. ^{1}H NMR (400.132 MHz, CD_2Cl_2): δ 1.13 (t+d, 6H, $^{3}J_{H-H}$ = 7.9 Hz, $^{2}J_{Pt-H}$ = 84.8 Hz, $PtCH_2CH_3$), 1.78 (q+d, 4H, $^{3}J_{H-H}$ = 7.9 Hz, $^{2}J_{Pt-H}$ = 89.4 Hz, $PtCH_2CH_3$), 7.67 (dd, 2H, bpym $H_{5/5'}$), 9.29 (dd, 2H, bpym $H_{4/4'}$), 9.37 (dd+dd, 2H, $^{3}J_{Pt-H}$ = 18.0 Hz, bpym $H_{6/6'}$). ^{13}C{^{1}H} NMR (100.623 MHz, CD_2Cl_2): δ −0.95 (s+d, $^{1}J_{Pt-C}$ = 890.0 Hz, $-CH_2CH_3$), 17.9 (s+d, $^{2}J_{Pt-C}$ = 40.1 Hz, $-CH_2CH_3$), 124.6 (s+d, $^{3}J_{Pt-C}$ = 12.9 Hz, bpym $C_{5/5'}$), 153.6 (s+d, $^{2}J_{Pt-C}$ = 25.4 Hz, bpym $C_{6/6'}$), 156.9 (s, bpym $C_{4/4'}$), 163.2 (s, bpym $C_{2/2'}$). HRMS(ESI): calcd for [M−Et]$^+$ 382.0632, found 382.0633.

Preparation of (bpym)Pt(Et)(TFA), 2. HTFA (37 mL, 0.486 mmol) was dissolved in 3 mL of CH_2Cl_2 and added dropwise to a solution containing 200 mg (0.486 mmol) of Pt(bpym)(CH_2CH_3)$_2$ in 25 mL of CH_2Cl_2 at −78 °C. The red solution slowly changed to an orange solution during addition of the acid, accompanied by gas evolution. The reaction mixture was allowed to warm to room temperature. The solution was concentrated (ca. ∼5 mL) using a rotary evaporator, and 30 mL of pentane was added to precipitate an orange solid. The solid was centrifuged, and the supernatant was removed and dried using high vacuum to give a 91% yield. ^{1}H NMR (400.132 MHz, CD_2Cl_2): δ 0.86 (t+m, 3H, $^{3}J_{H-H}$ = 7.6 Hz,), 1.85 (q +d, 2H, $^{3}J_{H-H}$ = 7.6 Hz, $^{2}J_{Pt-H}$ = 86.2 Hz, $PtCH_2CH_3$), 7.65 (dd, 1H, bpym $H_{5/5'}$), 7.79 (dd, 1H, bpym $H_{5/5'}$), 8.88 (dd, 1H, bpym $H_{4/4'}$), 9.17−9.40 (m+m, 3H, $H_{4/4'}$, bpym $H_{6/6'}$, Pt-bpym $H_{6/6'}$). ^{13}C{^{1}H} NMR (100.623 MHz, CD_2Cl_2): δ 1.66 (s+d, $^{1}J_{Pt-C}$ = 784.4 Hz, $-CH_2CH_3$), 16.3 (s+d, $^{1}J_{Pt-C}$ = 32.9 Hz, $-CH_2CH_3$), 116.0 (q, $-OCOCF_3$, $^{1}J_{C-F}$ = 289.7 Hz), 124.7 (s+d, $^{3}J_{Pt-C}$ = 47.3 Hz, bpym $C_{4/4'}$), 125.3 (s, bpym), 154.9 (s, bpym), 156.5 (s+d, $^{4}J_{Pt-C}$ = 37.3 Hz, bpym), 157.9 (s, bpym), 159.8 (s, bpym), 160.8 (s, bpym $C_{2/2'}$), 162.9 (q, $-OCOCF_3$, $^{2}J_{C-F}$ = 36.4 Hz), 164.2 (s, bpym $C_{2/2'}$). ^{19}F NMR (376.461 MHz, CD_2Cl_2): δ −74.7 (s+d, $-OCOCF_3$, $^{4}J_{Pt-F}$ = 19.5 Hz, Pt-$OCOCF_3$). HRMS(ESI): calcd for [M−TFA]$^+$ 382.0632, found 382.0631. Anal. Calcd for $C_{11}H_9F_3N_4O_2Pt$ (M_r = 495.32): C, 29.10; H, 2.24; N, 11.31. Found: C, 29.37; H, 2.45; N, 11.25. X-ray-quality orange needles of Pt(bpym)(Et)(TFA)·CH_2Cl_2 were obtained by crystallization from dichloromethane.

Experimental Procedures. *General Procedure for Ethane Oxidation to Ethanol and Isethioinic Acid.* In a typical experiment, a 15 mL stainless steel reactor with a glass or PTFE insert and a cross stir bar was loaded with 3 mL of a 15 mM solution of Pt(bpym)$(TFA)_2$ in either 98% H_2SO_4 or 101% H_2SO_4. The reactor was sealed and flushed with 500 psi of ethane (five times) while the solution was stirred. The reactor was then pressurized with 500 psi of ethane and sealed. It was placed on a preheated aluminum block maintained by a temperature controller at the desired reaction temperature (160 °C). Next, the reactor was then heated for 1 h while stirring continued at 1000 rpm. After the reaction, the reactor was removed from the aluminum block and the reaction quenched by placing the reactor in a dry ice/acetone bath until cooled to room temperature. Headspace analyses were performed by venting the reactor into an evacuated, septa-capped 30 mL vial with an outlet connected to a one-way gas check valve and analyzing the gas phase by GC-MS using neon as an internal standard. Liquid-phase analysis was performed by opening the reactor, adding 50 μL of HOAc or MeOH as an internal standard, and taking a 0.6 mL aliquot for analysis by ^{1}H and ^{13}C NMR utilizing a C_6D_6 external capillary. Yields of isethionic acid (ITA) were determined by comparison of the integration values of HOAc to the two triplets of ITA, which were averaged prior to calculation of yield.

Stoichiometric Reactions of Model Complexes. The stoichiometric reactions were carried out by directly injecting 0.1 mL of a 0.52 M solution of the model Pt-Et (or Pt-Me) complex in DMSO all at once into a magnetically stirred 8 mL glass vial, equipped with a Teflon seal, containing 5 mL of concentrated H_2SO_4 or HOTf, and heated to a 160 °C on an aluminum block. Upon addition of the solution, the vial was immediately removed and cooled in a dry ice bath, and 2.5 mL of methane (or ethane for Pt-Me) and 5 μL of AcOH were added via syringe as gas and liquid standards, respectively. The liquid and gas phases were then sampled and analyzed as described above. Control experiments showed that the DMSO solvent is stable for the time scale of the reaction described above and did not generate any C_2 or C_1 products in the presence or absence of the Pt complex **1**. The reaction mixtures remained homogeneous and light orange, and no solids were observed.

Determination of SO_2 Generated from Pt^{II}-X. The SO_2 reactions were carried out in duplicate by directly injecting 0.1 mL of a 0.52 M solution of the model Pt-Et (**2**), Pt-Me (**3**), or **1** (as a "background") in DMSO all at once into a magnetically stirred 8 mL glass vial, equipped with a Teflon seal, containing 5 mL of concentrated H_2SO_4 or HOTf, and heated to a 160 °C with an aluminum block. Upon addition of the solution, the vial was immediately removed and cooled in a dry ice bath until cool to the touch. To the vials containing Pt-Et were added 2.5 mL of methane (or ethane for the vials containing Pt-Me) and 5 μL of AcOH as gas and liquid standards, respectively. The second vial was cooled in an ice bath to lower the vapor pressure of the solvent. The Teflon seal was pierced with a cannula, the other end of

dx.doi.org/10.1021/ja504368r | J. Am. Chem. Soc. XXXX, XXX, XXX−XXX

which was immersed in a stirred solution of 10 mL of 0.3% H_2O_2(aq) with a few drops of bromothymol blue (as a pH indicator). Bubbling was observed, with an instantaneous color change of the solution (to yellow, indicating an acidic shift in pH) upon piercing the Teflon septum. An additional needle was inserted into the reaction vial with constant flowing N_2. After 10 min of sparging the solution, the flow was stopped. The solution containing H_2O_2 and indicator was back-titrated with a 0.01 M solution of KOH(aq) until it returned to basic (blue in color). The SO_2 obtained in the H_2SO_4 runs correlated with product observed in the liquid phase. The background reaction (with **1**) showed no detectable concentration of SO_2. No SO_2 was observed from the HOTf reactions.

Determination of SO_2 Generated from Catalytic Reaction. The test utilized for the stoichiometric reaction was used, except the catalytic reactor was vented into the H_2O_2 solution containing of bromothymol blue (as a pH indicator).

Details of Computational Analysis. All calculations were carried out in Gaussian 09.[62] Geometries were optimized with the B3LYP/6-31G(d,p)[LANL2DZ] functional.[63] B3LYP enthalpy and entropy corrections were used for all thermodynamic corrections. B3LYP and M06[64] energies were further refined with the 6-311+G(2d,p)/LANL2TZ(f) and 6-311++G(2df,2dp)/LANL2TZ(f) basis sets. Solvation was treated using the SMD[65] polarizable continuum model augmented for H_2SO_4 (see SI).

■ ASSOCIATED CONTENT

Supporting Information

Additional experimental procedures, computational methods, and X-ray crystallographic data. This material is available free of charge via the Internet at http://pubs.acs.org.

■ AUTHOR INFORMATION

Corresponding Authors

bhashigu@scripps.edu
dhe@chem.byu.edu
rperiana@scripps.edu

Notes

The authors declare no competing financial interest.

■ ACKNOWLEDGMENTS

This work was supported as part of the Center for Catalytic Hydrocarbon Functionalization, an Energy Frontier Research Center Funded by the U.S. Department of Energy, Office of Science, Office of Basic Energy Sciences, under award no. DE-SC0001298 (to R.A.P. and D.H.E.).

■ REFERENCES

(1) U.S. Energy Information Administration. U.S. Crude Oil and Natural Gas Proved Reserves, 2011, 2013.
(2) George, D. L.; Bowles, E. B., Jr. *Pipeline Gas J.* **2011**, *238*, 38.
(3) Haggin, J. *Chem. Eng. News* **1993**, *71* (34), 21−22.
(4) Periana, R. A.; Bhalla, G.; Tenn, W. J.; Young, K. J. H.; Liu, X. Y.; Mironov, O.; Jones, C. J.; Ziatdinov, V. R. *J. Mol. Catal. A-Chem.* **2004**, *220*, 7.
(5) Conley, B. L.; Tenn, W. J.; Young, K. J. H.; Ganesh, S. K.; Meier, S. K.; Ziatdinov, V. R.; Mironov, O.; Oxgaard, J.; Gonzales, J.; Goddard, W. A.; Periana, R. A. *J. Mol. Catal. A-Chem.* **2006**, *251*, 8.
(6) Shilov, A. E.; Shul'pin, G. B. *Chem. Rev.* **1997**, *97*, 2879.
(7) Chepaikin, E. G. *Russ Chem. Rev.* **2011**, *80*, 363.
(8) Lersch, M.; Tilset, M. *Chem. Rev.* **2005**, *105*, 2471.
(9) Crabtree, R. H. *J. Chem. Soc., Dalton Trans.* **2001**, 2951.
(10) Schwarz, H. *Angew. Chem., Int. Ed.* **2011**, *50*, 10096.
(11) Hashiguchi, B. G.; Bischof, S. M.; Konnick, M. M.; Periana, R. A. *Acc. Chem. Res.* **2012**, *45*, 885.
(12) Periana, R. A.; Taube, D. J.; Gamble, S.; Taube, H.; Satoh, T.; Fujii, H. *Science* **1998**, *280*, 560.
(13) Gol'dshleger, N. F.; Es'kova, V. V.; Shteinman, A. A.; Shilov, A. E. *Russ J. Phys. Ch. USSR* **1972**, *46*, 785.
(14) Chen, G. S.; Labinger, J. A.; Bercaw, J. E. *Proc. Natl. Acad. Sci. U.S.A.* **2007**, *104*, 6915.
(15) Labinger, J. A.; Bercaw, J. E. *Nature* **2002**, *417*, 507.
(16) Rostovtsev, V. V.; Labinger, J. A.; Bercaw, J. E.; Lasseter, T. L.; Goldberg, K. I. *Organometallics* **1998**, *17*, 4530.
(17) Stahl, S. S.; Labinger, J. A.; Bercaw, J. E. *J. Am. Chem. Soc.* **1995**, *117*, 9371.
(18) Stahl, S. S.; Labinger, J. A.; Bercaw, J. E. *J. Am. Chem. Soc.* **1996**, *118*, 5961.
(19) Fekl, U.; Goldberg, K. I. *Adv. Inorg. Chem.* **2003**, *54*, 259.
(20) Pawlikowski, A. V.; Getty, A. D.; Goldberg, K. I. *J. Am. Chem. Soc.* **2007**, *129*, 10382.
(21) Khusnutdinova, J. R.; Zavalij, P. Y.; Vedernikov, A. N. *Organometallics* **2007**, *26*, 3466.
(22) Vedernikov, A. N. *Curr. Org. Chem.* **2007**, *11*, 1401.
(23) Vedernikov, A. N.; Binfield, S. A.; Zavalij, P. Y.; Khusnutdinova, J. R. *J. Am. Chem. Soc.* **2006**, *128*, 82.
(24) Yahav-Levi, A.; Goldberg, I.; Vigalok, A.; Vedernikov, A. N. *J. Am. Chem. Soc.* **2008**, *130*, 724.
(25) Baik, M. H.; Newcomb, M.; Friesner, R. A.; Lippard, S. J. *Chem. Rev.* **2003**, *103*, 2385.
(26) Sen, A. *Acc. Chem. Res.* **1998**, *31*, 550.
(27) Butikofer, J. L.; Parson, T. G.; Roddick, D. M. *Organometallics* **2006**, *25*, 6108.
(28) Periana, R. A.; Mironov, O.; Taube, D.; Bhalla, G.; Jones, C. J. *Science* **2003**, *301*, 814.
(29) Periana, R. A.; Taube, D. J.; Evitt, E. R.; Loffler, D. G.; Wentrcek, P. R.; Voss, G.; Masuda, T. *Science* **1993**, *259*, 340.
(30) Zerella, M.; Mukhopadhyay, S.; Bell, A. T. *Chem. Commun.* **2004**, 1948.
(31) De Vos, D. E.; Sels, B. E. *Angew. Chem., Int. Ed.* **2005**, *44*, 30.
(32) Mironov, O. A.; Bischof, S. M.; Konnick, M. M.; Hashiguchi, B. G.; Ziatdinov, V. R.; Goddard, W. A., III; Ahlquist, M.; Periana, R. A. *J. Am. Chem. Soc.* **2013**, *135*, 14644.
(33) Lodgsdon, J. E. In *Encyclopedia of Chemical Technology 9*, 4th ed.; Howe-Grant, M., Kirk, R. E., Othmer, D. F., Kroschwitz, J. I., Eds.; Wiley: New York, 1991; p 817.
(34) Labinger, J. A. In *Alkane C-H Activation by Single-Site Metal Catalysis*; Pérez, P. J., Ed.; Springer: New York, 2012; Vol. *38*, p 17.
(35) Kosswig, K. *Ullmann's Encyclopedia of Industrial Chemistry*; Wiley-VCH: Weinheim, 2000; Vol. *A25*, p 747.
(36) Kosswig, K. *Ullmann's Encyclopedia of Industrial Chemistry*; Wiley-VCH: Weinheim2000; Vol. *A25*, p 503.
(37) Brooks, B. T.; Humphrey, I. *J. Am. Chem. Soc.* **1918**, *40*, 822.
(38) Michael, A.; Weiner, N. *J. Am. Chem. Soc.* **1936**, *58*, 294.
(39) Bordwell, F. G.; Suter, C. M.; Webber, A. J. *J. Am. Chem. Soc.* **1945**, *67*, 827.
(40) Bordwell, F. G.; Rondestvedt, C. S. *J. Am. Chem. Soc.* **1948**, *70*, 2429.
(41) Bordwell, F. G.; Peterson, M. L. *J. Am. Chem. Soc.* **1954**, *76*, 3952.
(42) Bordwell, F. G.; Peterson, M. L. *J. Am. Chem. Soc.* **1954**, *76*, 3957.
(43) Bordwell, F. G.; Peterson, M. L.; Rondestvedt, C. S. *J. Am. Chem. Soc.* **1954**, *76*, 3945.
(44) Sen, A.; Benvenuto, M. A.; Lin, M. R.; Hutson, A. C.; Basickes, N. *J. Am. Chem. Soc.* **1994**, *116*, 998.
(45) Bass, S. J.; Gillespie, R. J.; Robinson, E. A. *J. Chem. Soc.* **1960**, 821.
(46) Gillespie, R. J. *J. Chem. Soc.* **1950**, 2493.
(47) Gillespie, R. J.; Robinson, E. A.; Solomons, C. *J. Chem. Soc.* **1960**, 4320.
(48) Basickes, N.; Hogan, T. E.; Sen, A. *J. Am. Chem. Soc.* **1996**, *118*, 13111.
(49) Crabtree, R. H. *The Organometallic Chemistry of the Transition Metals*, 5th ed.; John Wiley & Sons, Inc.: Hoboken, NJ, 2009.

(50) Collman, J. P.; Hegedus, L. S.; Norton, J. R.; Finke, R. G. *Principles and Applications of Organotransition Metal Chemistry*; University Science Books: Sausalito, CA, 1987.
(51) Dobereiner, G. E.; Crabtree, R. H. *Chem. Rev.* **2010**, *110*, 681.
(52) Attempts at directly comparing H/D exchange rates versus functionalization rates of ethane and methane through a competition experiment in D_2SO_4 were unsuccessful due to deuterium incorporation into $EtOSO_3H$ and CH_3OSO_3H in the presence and absence of the catalyst as well as multiple H/D exchange for every CH activation of the alkanes. See ref 34.
(53) Gilbert, T. M.; Hristov, I.; Ziegler, T. *Organometallics* **2001**, *20*, 1183.
(54) Hristov, I. H.; Ziegler, T. *Organometallics* **2003**, *22*, 1668.
(55) Paul, A.; Musgrave, C. B. *Organometallics* **2007**, *26*, 793.
(56) Ahlquist, M.; Periana, R. A.; Goddard, W. A. *Chem. Commun.* **2009**, 2373.
(57) Kiernan, P. M.; Ludi, A. *J. Chem. Soc., Dalton Trans.* **1978**, 1127.
(58) Connick, W. B.; Marsh, R. E.; Schaefer, W. P.; Gray, H. B. *Inorg. Chem.* **1997**, *36*, 913.
(59) Bruce, J.; Johnson, D.; Cordes, W.; Sadoski, R. *J. Chem. Crystallogr.* **1997**, *27*, 695.
(60) Clark, H. C.; Manzer, L. E. *J. Organomet. Chem.* **1973**, *59*, 411.
(61) Shiotsuki, M.; White, P. S.; Brookhart, M.; Templeton, J. L. *J. Am. Chem. Soc.* **2007**, *129*, 4058.
(62) Frisch, M. J.; Trucks, G. W.; Schlegel, H. B.; Scuseria, G. E.; Robb, M. A.; Cheeseman, J. R.; Scalmani, G.; Barone, V.; Menucci, B.; Petersson, G. A.; Nakatsuji, H.; Caricato, M.; Li, X.; Hratchian, H. P.; Izmaylov, A. F.; Bloino, J.; Zheng, G.; Sonnenberg, J. L.; Hada, M.; Ehara, M.; Toyota, K.; Fukuda, R.; Hasegawa, J.; Ishida, M.; Nakajima, T.; Honda, Y.; Kitao, O.; Nakai, H.; Vreven, T.; Montgomery, J. A., Jr.; Peralta, J. E.; Ogliaro, F.; Bearpark, M.; Heyd, J. J.; Brothers, E.; Kudin, K. N.; Staroverov, V. N.; Kobayashi, R.; Normand, J.; Raghavachari, K.; Rendell, A.; Burant, J. C.; Iyengar, S. S.; Tomassi, J.; Cossi, M.; Rega, N.; Millam, N. J.; Klene, M.; Knox, J. E.; Cross, J. B.; Bakken, V.; Adamo, C.; Jaramillo, J.; Gomperts, R.; Stratmann, R. E.; Yazyev, O.; Austin, A. J.; Cammi, R.; Pomelli, C.; Ochterski, J. W.; Martin, R. L.; Morokuma, K.; Zakrzewski, V. G.; Voth, G. A.; Salvador, P.; Dannenberg, J. J.; Dapprich, S.; Daniels, A. D.; Farkas, Ö.; Foresman, J. B.; Ortiz, J. V.; Cioslowski, J.; Fox, D. J. *Gaussian 09*, Revision B.01; Gaussian, Inc.: Wallingford, CT, 2009.
(63) Becke, A. D. *J. Chem. Phys.* **1993**, *98*, 5648.
(64) Zhao, Y.; Truhlar, D. G. *Theor. Chem. Acc.* **2008**, *120*, 215.
(65) Marenich, A. V.; Cramer, C. J.; Truhlar, D. G. *J. Phys. Chem. B* **2009**, *113*, 6378.